Temperature-invariant Casimir–Polder forces despite large thermal photon numbers

Simen Å. Ellingsen,[1] Stefan Yoshi Buhmann,[2] and Stefan Scheel[2]

[1] *Department of Energy and Process Engineering, Norwegian University of Science and Technology, N-7491 Trondheim, Norway**

[2] *Quantum Optics and Laser Science, Blackett Laboratory, Imperial College London, Prince Consort Road, London SW7 2AZ, United Kingdom*

(Dated: March 5, 2010)

We demonstrate that Casimir–Polder potentials can be entirely independent of temperature even when allowing for the thermal photon numbers to become large at the relevant molecular transition frequencies. This statement holds for potentials that are due to low-energy transitions of a molecule placed near a plane metal surface. For a molecule in an energy eigenstate, the temperature-invariance is a consequence of strong cancellations between nonresonant potential components and those due to evanescent waves. For a molecule with a single dominant transition in a thermal state, upward and downward transitions combine to a temperature-independent potential. The results are contrasted with the case of an atom whose potential exhibits a regime of linear temperature-dependence. Contact to the Casimir force between a weakly dielectric and a metal plate is made.

PACS numbers: 31.30.jh, 12.20.–m, 34.35.+a, 42.50.Nn

arXiv:1003.1261v1 [quant-ph] 5 Mar 2010

Dispersion forces between polarisable objects were originally predicted by Casimir and Polder as a consequence of quantum zero-point fluctuations [1, 2]. Recent measurements of both Casimir–Polder (CP) forces between atoms and surfaces [3] and Casimir forces between macroscopic bodies [4, 5] typically operate at room temperature where thermal fluctuations also come into play [6–9]. The temperature-dependence of dispersion forces is of relevance for both fundamental and practical reasons.

On the theoretical side, the correct description of the Casimir force between metals at finite temperature is subject to an ongoing debate [5, 10]. To wit, predictions differ for the high-temperature behaviour of the Casimir force between metals, for which employing a standard dissipative description of the surfaces fails to reproduce the experimental observations [11]. This suggests that progress can be made by directly observing the variation of the Casimir force with temperature.

On the practical side, CP forces become increasingly relevant when trying to trap and coherently manipulate cold atoms near surfaces [12]. Current endeavours aim at extending these techniques to more complex systems such as polar molecules [13]. Such systems typically exhibit long-wavelength transitions so that CP forces become increasingly long-ranged. This raises the question whether they can be controlled by lowering the ambient temperature and hence suppressing thermal force components.

Thermal contributions to the CP potential are governed by the photon number $n(\omega) = [\mathrm{e}^{\hbar\omega/(k_\mathrm{B}T)} - 1]^{-1}$. A noticeable deviation of the potential from its zero-temperature value is to be expected when $n(\omega) \gtrsim 1$ in the relevant frequency range. This is the case, for instance, for molecules with small transition frequencies, $|\omega_{kn}| \lesssim k_\mathrm{B}T/\hbar = 3.93 \times 10^{13}\,\mathrm{rad/s}$ at room temperature (300 K). The associated wavelengths are much larger than typical experimental molecule–surface separations in the nanometre to micrometre range [3], $z_\mathrm{A} \ll c/|\omega_{kn}|$. Furthermore, experimental realisations typically involve conducting and thus highly reflecting metal surfaces with $|\varepsilon(\omega_{kn})| \gg 1$.

As we will show in this Letter, the above three conditions combined result in potentials which are independent of temperature over the entire range from zero to room temperature and beyond. We will first discuss the case of a molecule prepared in an energy eigenstate and then consider molecules at thermal equilibrium with their environment, comparing our results with those for atoms whose transitions involve higher energies.

Molecule vs. atom in an eigenstate. As shown in Ref. [14], the CP potential of a molecule prepared in an isotropic energy eigenstate $|n\rangle$ at distance z_A from the plane surface of a metal,

$$U_n(z_\mathrm{A}) = U_n^\mathrm{nr}(z_\mathrm{A}) + U_n^\mathrm{ev}(z_\mathrm{A}) + U_n^\mathrm{pr}(z_\mathrm{A}), \qquad (1)$$

naturally separates into three contributions: a non-resonant term U_n^nr due to virtual photons that is formally similar to that produced by Lifshitz theory [6], and a resonant contribution due to real photons which may be further split into contributions from evanescent (U_n^ev) and propagating (U_n^pr) waves. The non-resonant potential is given by [14]

$$U_n^\mathrm{nr}(z_\mathrm{A}) = -\frac{\mu_0 k_\mathrm{B}T}{6\pi\hbar} \sum_k |\boldsymbol{d}_{nk}|^2 {\sum_{j=0}^{\infty}}' \frac{\omega_{kn}}{\omega_{kn}^2 + \xi_j^2} \int_{\xi_j/c}^{\infty} \mathrm{d}b \times \mathrm{e}^{-2bz_\mathrm{A}} \left\{ 2b^2c^2 r_p(\mathrm{i}\xi_j) - \xi_j^2 [r_s(\mathrm{i}\xi_j) + r_p(\mathrm{i}\xi_j)] \right\} \qquad (2)$$

[$\omega_{kn} = (E_k - E_n)/\hbar$, transition frequencies; $\boldsymbol{d}_{nk}$, dipole matrix elements; $\xi_j = j\xi$ with $\xi = 2\pi k_\mathrm{B}T/\hbar$, Matsubara frequencies; the primed summation indicates that the

term $j=0$ carries half weight] and the evanescent one reads

$$U_n^{\rm ev}(z_{\rm A}) = \frac{\mu_0}{12\pi}\sum_k n(\omega_{kn})|\boldsymbol{d}_{nk}|^2\int_0^\infty {\rm d}b\,{\rm e}^{-2bz_{\rm A}}\big\{2b^2c^2 \times {\rm Re}[r_p(\omega_{kn})] + \omega_{nk}^2{\rm Re}[r_s(\omega_{kn})+r_p(\omega_{kn})]\big\}, \quad (3)$$

note that $n(\omega_{kn}) = -[n(\omega_{nk})+1]$ for downward transitions. These two contributions dominate in the region $z_{\rm A}|\omega_{kn}|/c \ll 1$ we are interested in, while the spatially oscillating $U_n^{\rm pr}$ becomes relevant only in the far-field range $z_{\rm A}|\omega_{kn}|/c \gg 1$. The reflection coefficients of the surface for s- and p-polarised waves are given by $r_s(\omega)=(b-b_1)/(b+b_1)$ and $r_p(\omega)=[\varepsilon(\omega)b-b_1]/[\varepsilon(\omega)b+b_1]$ with $b_1=\sqrt{b^2-[\varepsilon(\omega)-1]\omega^2/c^2}$, ${\rm Re}(b_1)>0$.

For a metal surface whose plasma frequency is typically much larger than the molecular transition frequency ω_{kn}, we have $|\varepsilon(\omega)|\gg 1$ in the relevant frequency range, so that the reflection coefficients $r_s\approx -1$ and $r_p\approx 1$ become frequency-independent. The b-integrals can then be performed to give

$$U_n^{\rm nr}(z_{\rm A}) = -\frac{k_{\rm B}T}{12\pi\varepsilon_0\hbar z_{\rm A}^3}\sum_k|\boldsymbol{d}_{nk}|^2{\sum_{j=0}}'\frac{\omega_{kn}{\rm e}^{-2jz_{\rm A}\xi/c}}{\omega_{kn}^2+j^2\xi^2} \times\left[1+2j\,\frac{z_{\rm A}\xi}{c}+2j^2\,\frac{z_{\rm A}^2\xi^2}{c^2}\right], \quad (4)$$

$$U_n^{\rm ev}(z_{\rm A}) = \frac{1}{24\pi\varepsilon_0 z_{\rm A}^3}\sum_k n(\omega_{kn})|\boldsymbol{d}_{nk}|^2. \quad (5)$$

The asymptotic temperature-dependence of the potential for a given distance from the surface is governed by two characteristic temperatures: The molecular transition frequency defines a spectroscopic temperature $T_\omega=\hbar|\omega_{kn}|/k_{\rm B}$, which is roughly the temperature required to noticeably populate the upper level. Similarly, the distance introduces a geometric temperature $T_z=\hbar c/(z_{\rm A}k_{\rm B})$, i.e., the temperature of radiation whose wavelength is of the order $z_{\rm A}$.

We will now show that the total potential becomes independent of temperature in both the geometric low-temperature limit $T\ll T_z$ and the spectroscopic high-temperature limit $T\gg T_\omega$. For a typical molecule with its long-wavelength transitions, the potential is nonretarded for typical molecule–surface distances, $z_{\rm A}|\omega_{kn}|/c\ll 1$. As depicted in Fig. 1(i), this implies $T_\omega\ll T_z$, hence the two regions of constant potential overlap and the potential is constant for all temperatures. For an atom, on the contrary, the transition wavelengths are much shorter, so that we may have $z_{\rm A}|\omega_{kn}|/c\gg 1$. In this case, an intermediate regime $T_z\ll T\ll T_\omega$ exists where the potential increases linearly with temperature, cf. Fig. 1(ii).

We begin with a typical molecule with $z_{\rm A}|\omega_{kn}|/c\ll 1$. In the geometric low-temperature limit $T\ll T_z$, we have $z_{\rm A}\xi/c\ll 1$, hence the sum in Eq. (4) is densely spaced. The factor $1/(\omega_{kn}^2+j^2\xi^2)$ restricts it to values where

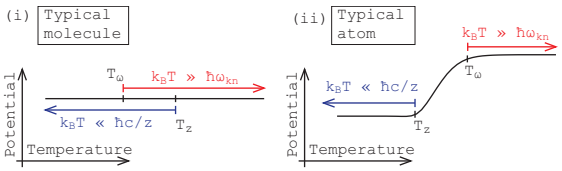

FIG. 1: Sketch of the temperature-dependence of the CP potential for a typical molecule vs. a typical atom.

$jz_{\rm A}\xi/c \le z_{\rm A}|\omega_{kn}|/c\ll 1$. With this approximation, the summation can be performed as

$${\sum_{j=0}}'\frac{1}{a^2+j^2} = \frac{\pi}{2a}\coth(\pi a) \quad (6)$$

and we find

$$U_n^{\rm nr}(z_{\rm A}) \overset{T\ll T_z}{=} -\frac{1}{24\pi\varepsilon_0 z_{\rm A}^3}\sum_k\left[n(\omega_{kn})+\tfrac{1}{2}\right]|\boldsymbol{d}_{nk}|^2, \quad (7)$$

noting that $\coth[\hbar\omega_{kn}/(2k_{\rm B}T)] = 2n(\omega_{kn})+1$. Adding the evanescent contribution (5), we find the temperature-independent total potential

$$U_n(z_{\rm A}) \overset{T\ll T_z}{=} -\frac{\sum_k|\boldsymbol{d}_{nk}|^2}{48\pi\varepsilon_0 z_{\rm A}^3} = -\frac{\langle\hat{\boldsymbol{d}}^2\rangle_n}{48\pi\varepsilon_0 z_{\rm A}^3}, \quad (8)$$

in agreement with the well-known nonretarded zero-temperature result [1].

In the spectroscopic high-temperature limit $T\gg T_\omega$, we have $\xi/|\omega_{kn}|\gg 1$. Due to the denominator $\omega_{kn}^2+j^2\xi^2$, the $j=0$ term strongly dominates the sum in Eq. (4) and we find

$$U_n^{\rm nr}(z_{\rm A}) \overset{T\gg T_\omega}{=} -\frac{1}{24\pi\varepsilon_0 z_{\rm A}^3}\sum_k\frac{k_{\rm B}T}{\hbar\omega_{kn}}|\boldsymbol{d}_{nk}|^2. \quad (9)$$

Under the condition $T\gg T_\omega$, i.e., $k_{\rm B}T\gg\hbar|\omega_{kn}|$, the evanescent contribution (5) reduces to

$$U_n^{\rm ev}(z_{\rm A}) \overset{T\gg T_\omega}{=} \frac{1}{24\pi\varepsilon_0 z_{\rm A}^3}\sum_k\left(\frac{k_{\rm B}T}{\hbar\omega_{kn}}-\frac{1}{2}\right)|\boldsymbol{d}_{nk}|^2. \quad (10)$$

Adding the two results, the total potential is again temperature-independent and given by Eq. (8). This limit is just the high-temperature saturation already pointed out in Refs. [8, 14].

The thermal CP potential of a typical molecule with its long-wavelength transitions has thus been found to be temperature-invariant in the geometric low-temperature and spectroscopic high-temperature regimes. Due to the condition $z_{\rm A}|\omega_{kn}|/c\ll 1$, at least one of the conditions $T\ll T_z$ or $T\gg T_\omega$ always holds, implying that the potential is constant for all temperatures and it agrees with its zero-temperature value. The invariance of the total potential in both regimes is a result of cancellations between nonresonant and evanescent potential components, which

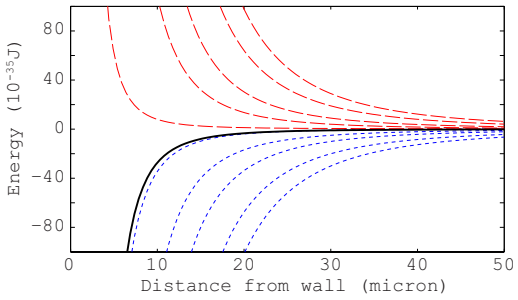

FIG. 2: CP potential of a ground-state LiH molecule in front of a Au surface. We show the total potential (solid line) as well as its evanescent (dashed) and nonresonant (dotted) contributions for temperatures 10K, 50K, 100K, 200K, 300K (left to right).

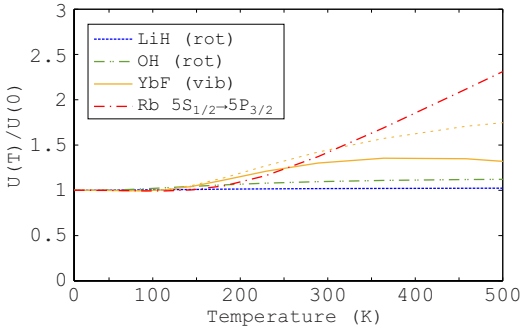

FIG. 3: Temperature-dependence of the CP potential of various ground-state atoms and molecules at distance $z_A = 5\mu$m from a Au surface. The transition frequencies of these species are such that $z_A\omega_{kn}/c$=0.046 (LiH), 0.26 (OH), 1.59 (YbF), 40.2 (Rb). For comparison, the perfect-conductor result for YbF is also shown (dotted line).

both strongly depend on temperature. This is illustrated in Fig. 2 where we display the total temperature-invariant potential as well as its nonresonant and evanescent parts for a ground-state LiH molecule in front of a Au surface for various temperatures. It is seen that very strong cancellations occur, especially at high temperatures.

We now turn to the case of atoms, whose electronic wavelengths are short compared to typical experimental separations: $z_A|\omega_{kn}|/c \gg 1$. The exponential restricts the sum in Eq. (4) to terms with $j\xi \lesssim c/z_A \ll |\omega_{kn}|$, so the term $j^2\xi^2$ in the denominator may be neglected. The sum can then be performed according to

$$\sum_{j=0}^{\infty}{}' e^{-2ja}(1+2ja+2j^2a^2) = \frac{\coth(a)}{2} + \frac{a}{2}\frac{1+a\coth(a)}{\sinh^2(a)} \to \begin{cases} 3/(2a), & a \ll 1; \\ 1/2, & a \gg 1. \end{cases} \quad (11)$$

In the geometric low-temperature regime, $T \ll T_z$, we further have $z_A\xi/c \ll 1$, i.e., $a \ll 1$ in Eq. (11), hence

$$U_n^{\rm nr}(z_A) \overset{T\ll T_z}{=} -\frac{c}{16\pi^2\varepsilon_0 z_A^4}\sum_k \frac{|\boldsymbol{d}_{nk}|^2}{\omega_{kn}}, \quad (12)$$

in agreement with the famous zero-temperature result of Casimir and Polder [1]. Moreover, the condition $z_A|\omega_{kn}|/c \gg 1$ implies that $T \ll T_z \ll T_\omega$: The geometric low-temperature regime is also a spectroscopic one and hence the evanescent potential reduces to

$$U_n^{\rm ev}(z_A) \overset{T\ll T_z}{=} -\frac{1}{24\pi\varepsilon_0 z_A^3}\sum_k \Theta(\omega_{nk})|\boldsymbol{d}_{nk}|^2. \quad (13)$$

[$\Theta(x)$, unit step function]. Adding the two contributions, we find the temperature-independent total potential

$$U_n(z_A) \overset{T\ll T_z}{=} -\frac{1}{24\pi\varepsilon_0 z_A^3}\sum_k \left[\frac{3c}{2z_A\omega_{kn}} + \Theta(\omega_{nk})\right]|\boldsymbol{d}_{nk}|^2 \quad (14)$$

in the geometric low-temperature regime.

For intermediate temperatures $T_z \ll T \ll T_\omega$ we have $z_A\xi/c \ll 1$, so using $a \gg 1$ in the sum (11), the nonresonant potential (4) is found to read as in Eq. (9). The evanescent contribution is still given by Eq. (13), so the total potential varies linearly with temperature,

$$U_n(z_A) \overset{T_z\ll T\ll T_\omega}{=} -\frac{1}{24\pi\varepsilon_0 z_A^3}\sum_k \left[\frac{k_B T}{\hbar\omega_{kn}} + \Theta(\omega_{nk})\right]|\boldsymbol{d}_{nk}|^2. \quad (15)$$

In the spectroscopic high-temperature limit $T \gg T_\omega$, the evanescent contribution is given by Eq. (10) as already shown. It cancels with the nonresonant contribution, still agreeing with Eq. (9), to give a saturated potential of the form (8). However, with, e.g., $T_\omega \approx 18.000$ K for Rb, this saturation is unobservable. Moreover, as the electronic transition frequencies can be comparable to the plasma frequency of the metal, the assumptions $r_s \approx -1$ and $r_p \approx 1$ do not hold. As a consequence, the cancellations required to achieve saturation do not occur for atoms near realistic metal surfaces.

We have thus seen that for an atom with $z_A|\omega_{kn}|/c \gg 1$, separate geometric low-temperature and spectroscopic high-temperature regimes exist, with the potential exhibiting a linear temperature-dependence between these two regions. The difference between the thermal CP potentials of typical atoms vs. molecules is illustrated in Fig. 3 where we show the temperature-dependence of the potential at fixed distance from a Au surface for different species. The potentials associated with the long-wavelength, rotational transitions of LiH and OH are virtually temperature-invariant while the short-wavelength electronic transition of Rb shows a linear increase over a large range of temperatures. YbF with its dominant vibrational transition lies in between the two extremes of typical long-wavelength molecular and short-wavelength atomic transitions; its potential increases by about 30%

in the displayed temperature range. In contrast to the other examples, the potential of YbF noticeably deviates from the corresponding ideal conductor-result due to imperfect reflection. Note that contributions to the molecular CP potentials due to electronic transitions are smaller than the rotational and vibrational ones (8) by factors $c/(z_{\rm A}\omega_{kn}) \ll 1$ (14) or $k_{\rm B}T/(\hbar\omega_{kn}) \ll 1$ (15) within the displayed temperature range and are hence negligible.

Molecule at thermal equilibrium. The proven temperature-invariance immediately generalises to molecules in incoherent superpositions of energy eigenstates with temperature-independent probabilities p_n and total potential $U(z_{\rm A}) = \sum_n p_n U_n(z_{\rm A})$. The case of a molecule at thermal equilibrium with its environment needs to be treated separately since the respective probabilities $p_n = \exp[-E_n/(k_{\rm B}T)]/\sum_k \exp[-E_k/(k_{\rm B}T)]$ depend on T. At thermal equilibrium, all resonant potential components cancel pairwise [9]. Introducing potential components U_{nk} due to a particular transition $n \leftrightarrow k$ (such that $U_n = \sum_k U_{nk}$) and the associated statistical weights $p_{nk} = p_n + p_k$, and exploiting the fact that $U_{kn} = -U_{nk}$, we can write the total potential in the form

$$\begin{aligned} U(z_{\rm A}) &= \sum_{n<k} (p_n - p_k) U^{\rm nr}_{nk}(z_{\rm A}) \\ &= \sum_{n<k} p_{nk} \tanh\left(\frac{\hbar\omega_{kn}}{2k_{\rm B}T}\right) U^{\rm nr}_{nk}(z_{\rm A}). \end{aligned} \tag{16}$$

The behaviour of this potential in the two limits relevant for a molecule with $z_{\rm A}|\omega_{kn}|/c \ll 1$ follow immediately from the asymptotes given in the previous section. For $T \ll T_z$, $U^{\rm nr}_{nk}$ from Eq. (7) leads to

$$U(z_{\rm A}) \overset{T\ll T_z}{=} -\frac{1}{48\pi\varepsilon_0 z_{\rm A}^3} \sum_{n<k} p_{nk} |\boldsymbol{d}_{nk}|^2, \tag{17}$$

where $n(\omega_{kn})+1/2 = \coth[\hbar\omega_{kn}/(2k_{\rm B}T)]/2$ has been used once more. For $T \gg T_\omega$, we recall $U^{\rm nr}_{nk}$ from Eq. (9) and note that $\tanh[\hbar\omega_{kn}/(2k_{\rm B}T)] \approx \hbar\omega_{kn}/(2k_{\rm B}T)$ to again find the potential (17).

Combining the two results, we may use the main argument of the previous section to conclude that the potential components associated with a particular transition $n \leftrightarrow k$ are independent of temperature for all temperatures. The invariance is a result of cancellations between the purely nonresonant contributions from lower state n and upper state k. For larger thermal photon numbers, these cancellations become stronger and hence counteract the increase of the potential one might have expected. Note however that the statistical weights p_{nk} introduce a weak temperature-dependence in general: The total potential is only strictly temperature-invariant when dominated by a single transition.

Relevance to Casimir forces. To illustrate the relevance of the demonstrated temperature-invariance to the Casimir force, let us consider an infinite dielectric half space filled with molecules of number density η at a distance z from a metal plane. For a weakly dielectric medium, the Casimir energy per unit area is given by $E(z) = \int_z^\infty {\rm d}z_{\rm A}\, \eta U(z_{\rm A})$ [15]. Using Eq. (17), we find that

$$E(z) = \frac{\eta}{96\pi\varepsilon_0 z^2} \sum_{n<k} p_{nk} |\boldsymbol{d}_{nk}|^2 \tag{18}$$

which is temperature-independent under the conditions mentioned above.

For dielectrics with a stronger response, manybody-effects will lead to temperature-dependent corrections of higher order in the molecular polarisability. Such corrections are suppressed in the spectroscopic high-temperature limit $T \gg T_\omega$, since they are of higher order in $\tanh[\hbar\omega_{kn}/(2k_{\rm B}T)] \ll 1$.

Summary. The demonstrated temperature-independence encountered for molecules with long-wavelength transitions shows that CP forces on such systems cannot be altered by adjusting the ambient temperature. Instead, the original zero-temperature results of Casimir and Polder apply universally across the whole temperature range. It is worth emphasising that a 'classical' regime of linear temperature-dependence is never reached. Our results further indicate that when accounting for the thermal excitation of the media, the temperature-dependence of Casimir forces involving dielectrics may be weaker than previously thought.

We have benefited from discussions with I. Brevik, A. Lambrecht and S. Reynaud. This work was supported by the UK Engineering and Physical Sciences Research Council. Support from the European Science Foundation (ESF) within the activity 'New Trends and Applications of the Casimir Effect' is gratefully acknowledged.

* Electronic address: simen.a.ellingsen@ntnu.no

[1] H.B.G. Casimir and D. Polder, Phys. Rev. **73**, 360 (1948);
[2] H.B.G. Casimir, Proc. K. Ned. Akad. Wet. **51**, 793 (1948).
[3] C.I. Sukenik *et al.*, Phys. Rev. Lett. **70**, 560 (1993); M. Marrocco, *et al.*, Phys. Rev. Lett. **81**, 5784 (1998); H. Failache, *et al.*, Phys. Rev. Lett. **83**, 5467 (1999); V. Druzhinina and M. DeKieviet, Phys. Rev. Lett. **91**, 193202 (2003): H. Kübler *et al.*, Nature Photon. **4**, 112 (2010).
[4] S. de Man *et al.*, Phys. Rev. Lett. **103**, 040402 (2009); F. Capasso *et al.*, IEEE J. Selec. Top. Quant. Electron. **13**, 400 (2007) and references therein.
[5] M. Bordag *et al.*, *Advances in the Casimir effect* (Oxford University Press, Oxford, 2009).
[6] E.M. Lifshitz, Zh. Eksp. Teor. Fiz. **29**, 94 (1955).
[7] T. Nakajima *et al.*, Phys. Rev. A **56**, 5100 (1997); S.-T. Wu and C. Eberlein, Proc. R. Soc. A **456**, 1931 (2000); Y. Sherkunov, Phys. Rev. A **79**, 032101 (2009).
[8] M.-P. Gorza and M. Ducloy, Eur. Phys. J. D **40**, 343 (2006).

[9] S.Y. Buhmann and S. Scheel, Phys. Rev. Lett. **100**, 253201 (2008).
[10] I. Brevik, *et al.*, New J. Phys. **8**, 236 (2006).
[11] R.S. Decca *et al.*, Ann. Phys. **318**, 37 (2005). **39**, 6945 (2006).
[12] Y.J. Lin *et al.*, Phys. Rev. Lett. **92**, 050404 (2004).
[13] J. van Veldhoven *et al.*, Phys. Rev. Lett. **94**, 083001 (2005).
[14] S.Å. Ellingsen *et al.*, Phys. Rev. A **79**, 052903 (2009).
[15] C. Raabe and D.-G. Welsch, Phys. Rev. A **73**, 063822 (2006).